International Research Journal of Engineering and Technology (IRJET) e-ISSN: 2395-0056
Volume: 07 Issue: 08 | Aug 2020 www.irjet.net p-ISSN: 2395-0072

Accurate Calculation of Noise Maps in GRAPPA using a *k*–space Analysis

Sindhu C[1], Narendra C P[2]

[1]PG Student, [2]Associate Professor
Dept. of Electronics and Communication Engineering, Bangalore Institute of Technology, Karnataka, India

---

Abstract - *Description of the noise scattering in Magnetic Resonance Images (MRI) will have numerous advantages, which includes standard assurance and protocol development. Noise description is a main key when similar imaging acceleration is present with multiple coil acquisitions, in which the noise dispersion can accommodate serious spatial heterogeneities. When parallel imaging regeneration is a direct procedure then, accurate noise study can be implemented by taking the correlations into considerations between all the samples that are involved. GRAPPA is a k–space based technique, in which the accurate examination has been considered statistically repressive since a large amount of noise covariance matrices are present. This is needed to descript the noise generation from k–space to frequency space (image–space). To keep away statistical load, GRAPPA reconstruction is formulated as a pixel wise linear process which was executed in the frequency space earlier. This methodology helps to evolve accurate description of bluster dispersal for self-calibrated similar with arbitrary Cartesian sampled pattern. By utilizing the symmetry and reparability generating noise operation, this methodology is statistically structured wherein any large matrices are useless. By estimating a fixed reconstruction kernel, error-free dispersal of the noise conflict for each coil's image can be achieved. Each coil noise maps are later merged accordingly to the coil merging proposal as in image regeneration, and can be appealed with complex coil merging and also with root sum-of-squares (SOS) approaches.*

Key Words: **Noise scattering, GRAPPA, image-space, *k*-space, interpolation, sum of squares and IFFT**

1. INTRODUCTION

Noise is basically a non-preventable origin of unwanted loss in MRI signals. The main origin of noise is the source, which is includes electrical bluster occurred throughout the addition of the sign in the output series. Noise destroys the optical standard from reformed images that is degraded which gets more complicated during post–processing techniques that is during segmenting, registering, fMRI inspection or approximation of framework numerically. Exact description variations in noise are necessary for quality assurance protocol optimization and also to customize post processing steps later. Practically, *k*–space noise is generally supposed as zero mean, dimensionally uncorrelated and IID complex Gaussian procedure for all coils, by providing uniform variation for imaginary and real portion. Suppose the information is provided by numerous output coils, multiple noise from coil can be represented from covariance matrix itself. The noise propagation in *k*–space into the image space can be expressed by matrix working in linear image regeneration. For completely sampling addition, the noise of IID bearing is conserved while transforming the information into the image space, which depends on the orthogonally of the Inverse Fast Fourier Transform (IFFT).

A g-factor otherwise called as general intelligence is the common mental capacity or general intellect factor. It is fluctuating that summarizes positive correlations among different rational task tends to be comparable. GRAPPA is a parallel imaging method to increase speed of MRI pulse series. The Fourier plane of the image is regenerated from the frequency signals of every coil. It is a method that regenerates the information in frequency domain. The GRAPPA directly distributes the g-factor GRAPPA. 2D or 3D Fourier transform of the MRI image that is measured is known as *K*-space. Its composite measurements are sampled during an MR measurement in a planned scheme managed by a pulse series that is an exactly timed series of radiofrequency and gradient pulses. Noise maps are the graphical depiction of the sound level dispersion and the generation of sound waves in a specified part for an assigned period. The main cause of noise in images are sensor illumination levels.

Avoiding the necessity of large covariance matrices: Complication of large covariance matrices is shortened by considering the *k*–space image reformation procedure for every multiplication of pixel, like in ***x***–space. Reformation in these methods give rise to statistical coherent noise description by preventing the large *k*–space correlations. Reformation from non-uniform *k*–space under-sampling will only be equalized for all location convolution, which involves misconception in the boundary in the middle of dissimilar locations.

1.1 Objectives of the Project

I. This paper purposes better than image–space and also methodical *k*–space noise generation analysis is been submitted. By considering entire correlations present in *k*–space, propagation of noise can be reconstructed.

II. Huge covariance matrices are taken away by utilizing large symmetries and separability in every the reformation step. This provides an accurate and arithmetically effective response to the noise dispersal in GRAPPA for each reformation channel and also describing noise in the last coil-merged image.

III. To provide accuracy under the supposition of stationary and un-correlation in the original under-sampled *k*-space acquisition.

IV. By complex or magnitude built coil merging methods, every coil images can be merged into magnitude complex image.

V. Every coil noise approximation are merged as stated to the chosen coil merging method, therefore specifying noise in the last merging images of coils. It will also assess the noise amplification (*g*-factor) in GRAPPA reformation.

1.2 Noise Characterization in GRAPPA

GRAPPA weights are non-stochastic as per the analysis because they are independent of the noise attainment. Which is absolutely correct only if they are approximated from a self-reliant acquisition. This estimation is expected to be a proper assumption also in self-calibrated additions only when classical determination of GRAPPA weight expected obtained regions in the k–space are identically distributed (IID). In spite of distinguishing the noise data in the finishing combined image, every steps of the GRAPPA processing will be correctly specified as mentioned in Figure 1.1. It shows a figured structure of the noise propagation throughout the whole GRAPPA regeneration algorithm. Through different channels the image is obtained and the representative *k*–space for every channel noise can be considered stationary, while correlations in the middle of channels exist. GRAPPA later regenerates the *k*–space for every channel by inserting the lost *k*–space locations.

Noise models inside the GRAPPA reformed pipeline with main noise parameters includes following steps

I. *k*–space Interpolation

II. Column iFFT

III. Row iFFT

IV. Coil combination

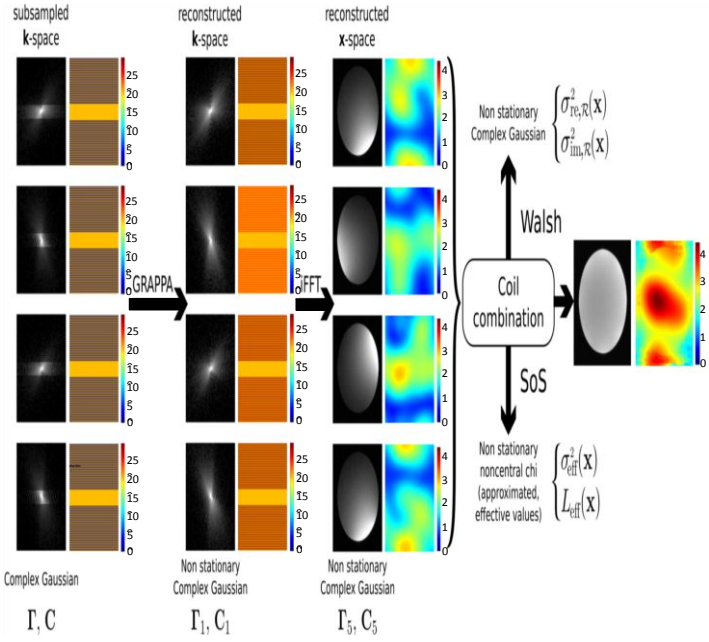

Fig 1.1: Noise models inside the GRAPPA

2. GRAPPA AND *K*-SPACE

2.1 GRAPPA

GRAPPA is the normalised execution of the VD-AUTO-SMASH. Unmerged images are formed for every coil present in the array to produce the lost lines for every coil in GRAPPA by applying multiple block wise reconstructions. This process as shown in Fig. 2.1

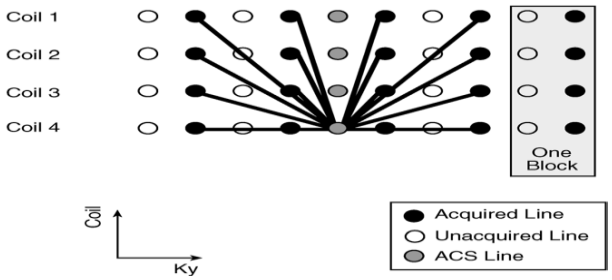

Fig. 2.1: The basic GRAPPA algorithm.

Black circles represent information gained in every coil array that are relevant to ACS lines represented by gray circles. Information from numerous line of entire coils are utilized to suit an ACS line in one coil, in such method an ACS lines from 4th coil. To generate the missing lines from that coil this fit provides the weights. FT is utilized to produce the non-merged images of particular coil when entire lines are regenerated for a specified coil. A complete group of unmerged images can be gained when this procedure is replicated for every coil of the array that are merged with the help of a normal sum of squares (SOS) technique.

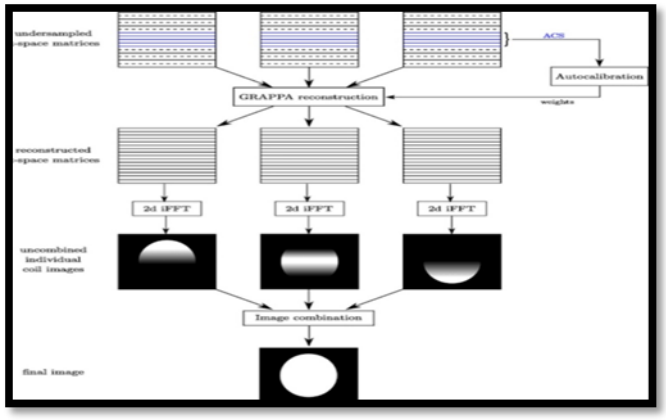

Fig 2.2: An overview of GRAPPA reconstruction algorithm in under-sampled *k*-space matrices

Firstly, under-sampled *k*-space matrices are turned into reconstructed *k*-space matrices by GRAPPA reconstruction algorithm along with the computation of ACS lines. These weights are then applied in the reconstruction step, which completes the missing lines in each coil matrix through 2D iFFT. Next, the individual coil images are generated and finally merged in image combination using sum of squares (SOS). Fig 2.2 shows the overview of GRAPPA reformation algorithm. The noise dispersal of the last composite image is based on the coil merging process that is used, here SOS procedure is used. GRAPPA weights are not irregular that is they are not dependent on the noise comprehension, this can be correct only when they are approximated from a individualistic acquisition. This estimation will be satisfying estimation in self-calibrated acquisitions also where in the obtained regions in the *k*-space are IID.

2.2 *K*-space

Assembling numbers corresponding to brightness represented by gray scale can be visualized on the display arranged typically in a square array or matrix form. To acquire a particular region of information rendering some property of anatomy or purpose a possible approach is required in imaging and also to utilize that information value to occupy the intensity on the image matrix. The X-ray film causes only half of the image regions to be gained which is the main problem, from the corresponding part of a control image obtained partial image would be proper and identical.

Mathematically, it is said that every single data regions and spatial regions contains each correspondence in middle of them. In MRI, the number of data regions is equal image regions represented as picture components and pixels since there is no correspondence to each pixel. Correspondingly, the whole image is determined by every data region that is obtained in some way but without all of the information or data the image cannot be fully reconstructed.

The neural networks are executed in the image field, by assembling multiple coil *k*-space information a proper neural network should be constructed in the *k*-space domain including the channel magnitude of the neural mesh. Deep neural network is instructed to know the relationship between the multiple coil *k*-space channel information and each channel reconstructed coil images as shown in Fig. 2.3.

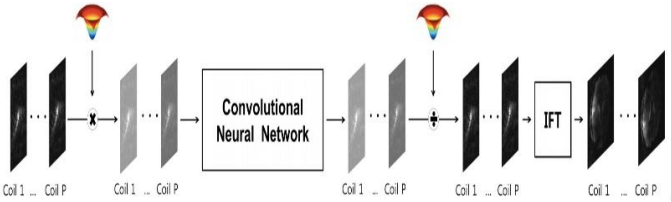

Fig. 2.3: The architecture of *k*-space

3. IMPLEMENTATION USING DATASETS

3.1 DATASETS

Three data sets are to be considered for the experiments namely,

I. Simulated Brain Dataset

II. Water Phantom Acquisition

III. In Vivo Acquisition

3.1.1 Simulated Brain Dataset:

SBD consists of group of practical MRI information volumes gained by an MRI simulator. These information are utilized by neuroimaging community to examine the production of other image analysis method in a situation in which the correctness can be known. Basically SBD will have information depending on two structural models, they are healthy general and Multiple Sclerosis (MS). For both models complete 3D information volume are restored utilizing three MRI series they are T1-, T2- and PD weighted.

From the above mentioned database a testimonial axial brain MR image is gained. For this proposed method T1-weighted image set to INU as 0%, with intensity non-uniform, slice thickness is set to 1mm and range of intensity generalized to [0,255]. By regulating the images utilizing artificial sensitive maps coding for every coil an 8 coil accession is restored. Coil images that are noise-free will be transformed into the *k*–space. Such transformed noise-free images are altered with synthetic Gaussian noise described from matrices Γ_k and C_k with SNR ranging to 30 for every coil. The correlation co-efficient in the middle of coils represented by ρ is set to 0.1. 4000 realizations of each image is used for statistical purpose.

3.1.2 Water Phantom Acquisition:

Water phantoms are the primary tool used for absolute dosimeter. Water phantoms are the model of a tissue which are economical, flexible and manageable tool to evolve imaging techniques. Water phantom are formed by water in volume ratio comparable to the tissue of clinical interest. 100 different realizations of completely encoding part of a water phantom is sedated using 4g/L of Sodium Chloride (NaCl) also 3.3685 g/L of Nickel Chloride Hydrate. On a 3.0T, two scanned 8-channel head coil scanner is present. TE/TR is 2.0/11.8ms, flip angle is 3°, view field is 220X220mm^2, matrix size is 128X128, slice thickness is 3mm, bandwidth is ±62.5KHz and complete scanning time is 641.2 seconds. 200 realizations are acquired in order to ensure steady-state and the first 100 realizations are discarded. Also B_0 domain drift connected to phase difference that is corrected from pre-processing steps that approximated the phases shifting.

3.1.3 In Vivo Acquisition

In vivo acquisition are datasets of that effects the various biological entities including cells, tissues of animals, plants and humans. In vivo are properly matched for noticing all the result of an experiment carried on an object. Completely encoded 2D axial slice head testing is performed to demonstrate the feasibility of the suggested technique that is used. Informed consent is gained earlier to the acquisition which was obtained with Fast Spin Echo (FSE) series utilizing a 32 channel head coils on a 3.0T scanner. TE/TR is ranged as 30.8/2000ms, field of view is 260X260mm^2, matrix size is 256X256, slice thickness is 3mm, bandwidth is ±22:5KHz and total scan time is 132 seconds.

3.2 EXPERIMENTS PERFORMED

Using data sets, three main experiments are performed in this proposed method namely,

I. Uniform Under-Sampling patterns.
II. Non-uniform subsampling patterns with ACS lines.
III. Non-uniform subsampling patterns with VD reconstruction.

3.2.1 Uniform Under-sampling Patterns

Under-sampling is a process in which a band-pass filtered signal is sampled at sampling rate which is less than Nyquist rate and reconstruction of the signal is possible. These are identical from the samples of a less frequency which is aliasing high frequency signal. With rectilinear sampling, uniform under-sampling will effect a simple aliasing pattern which allows resolving the reversed issues on a scale presented by the under sampling rate. Flatened sensing is necessary incoherence linking the sensing field and the object, in contrast to uniform under sampling. To increase encoding speed in MRI and also to imaging the dynamic objects uniform under sampling plays an important role.

Fig 3.1 shows the uniform under-sampling patterns. The image to be measured is denoted by m, which is the 2D-FT of the data denoted by d, in k-space. An under-sampling pattern is represented by the mask denoted as M. d_u represents under-sampled zero filled data set in k-space. The image reconstructed from the under-sampled data is denoted by m_u which is created through the 2D fourier transform of d_u. The reconstruction works because the fourier transform of M gives a near delta function which means no additional features are added to mu through the convolution. FFT *(M)* denotes the associated periodicity in its fourier transform. Eq (1) and (2) which are linked together through 2D fourier transforms.

$$d_u = M \text{ X } d \quad (1)$$

$$m_u = \text{F } (d)$$

$$m_u = \text{F } (M \text{ X } d)$$

$$m_u = \text{F } (M) * m \quad (2)$$

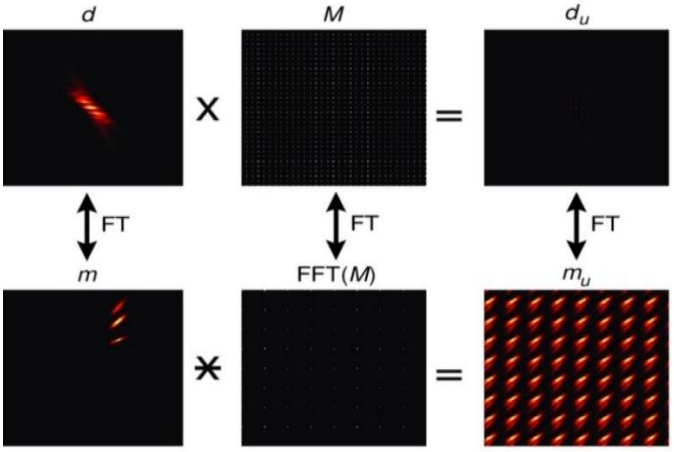

Fig 3.1: Uniform Under-sampling Patterns

As mentioned above uniform under-sampling patterns are known. When R = 2 and 32 ACS lines are present, the k–space information with respect to initial realization in every information set are subsampled. The GRAPPA kernel and the merging vector are approximated by ACS lines from the initial realization. The k–space information are under-sampled uniformly for every realization excluding ACS lines. The expectations underlying image space dependent techniques are true, hence image space techniques are almost equal to the proposed k–space technique for initial case. Hence there is zero delusion in the assumption of the g-factor maps. Fig 3.2 shows the uniform under-sampling pattern for simulated brain

dataset comparing different methods like Monte Carlo, *k*-space and Image-space.

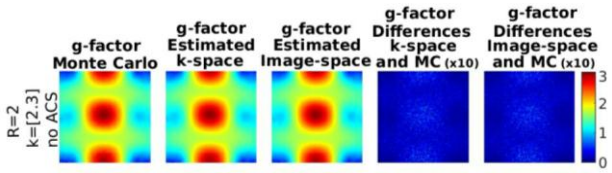

Fig 3.2: Uniform under-sampling pattern for simulated brain dataset

3.2.2 Non-Uniform Sub-sampling Patterns With ACS Lines

Sub-sampling reduces the image size by removing information all together. When subsampled, interpolation and also smoothing of image will also take place so that it will reduce aliasing. The chrominance values are filtered then subsampled by ½ or ¼ that of intensity. Sub-sampling includes, variance approximation and estimation of underlying distribution. Non-uniform sub-sampling allows to alter the sub-sampling method for revised image quality for large acceleration factors. Non-uniform sub-sampling includes fast regeneration methods like SENSE that helps in achieving regularized image than regeneration of the uniformly sub-sampled information requests. Non-uniform sub-sampling does automatic regularization and helps to get good image quality. Fig 3.3 shows the non-uniform sub-sampling patterns.

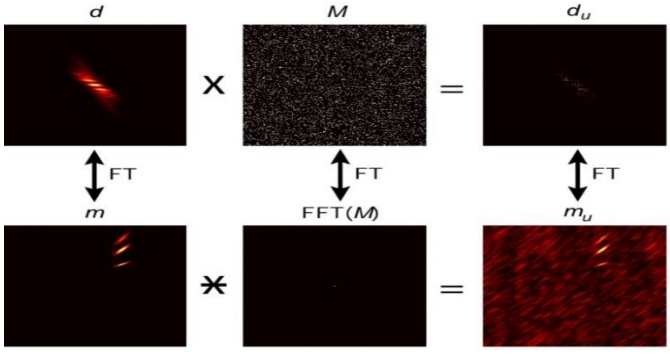

Fig 3.3: Non-Uniform sub-sampling Patterns

Auto Calibration Signals (ACS) are the signals that are compared between a known or a standard measurement and the measurement using the system. The accuracy standard measurement will be ten times better than that of a measuring signal. In non-uniform subsampling patterns in which ACS lines are present. Therefore, the *k*–space information for each realization and every individual information set are subsampled with an ACS location with 32 lines. Using three combinations of parameters the result of the kernel size and the acceleration size can be known. They are,

{R = 4; kernel = [3; 4]},
{R = 5; kernel = [3; 4]},
{R = 6; kernel = [5; 4]}.

For every experiment, the GRAPPA kernel and the coil merging vector are computed using those first realization of each data, later it is utilized to regenerate the last image. Fig 3.4 shows the non-uniform subsampling pattern for simulated brain dataset with 32 ACS lines.

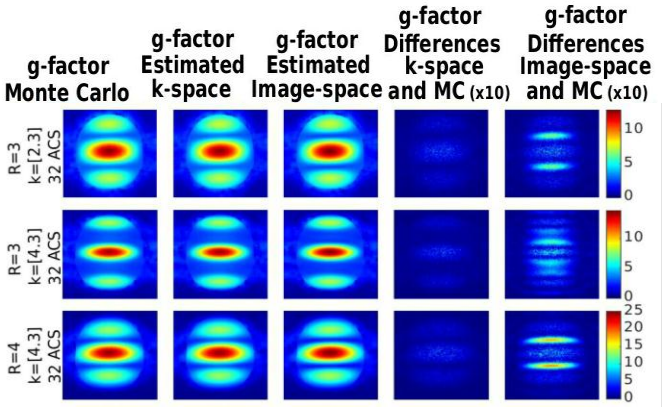

Fig 3.4: Non-uniform subsampling pattern with ACS lines for simulated brain dataset.

3.2.3 Non-Uniformly Sub-sampled Patterns With VD Reconstruction

Non-uniformly sub-sampled signals allows to alter the sub-sampling method for revised image quality for large acceleration factors. Non-uniform sub-sampling includes quick regeneration methods like SENSE and helps in achieving regularized image than reformation of the uniformly sub-sampled data request. Non-uniform sub-sampling does automatic regularization and helps to get good image quality.

Variable Density (VD) is a photographic soundtrack in which the signal is represented by a line of varying density. The proposed VD reconstruction helps in generating ensemble measurement which is computationally efficient and occupies less memory. Therefore VD reduces the necessary number of measurements for image reconstruction. VD can be applied to several transform domains which leads to simple implementations. Fig 3.5 shows the original image and VD reconstruction sampling image.

Fig 3.5: Original image and reconstruction from VD

In non-uniform subsampling patterns which is occurred by VD regeneration. In this method the initial image in every information set are subsampled by varying accelerating factor present in many *k*–space parts that is R=3, 4 and 5. And also un-accelerated location at the k–space center having 32 ACS lines. The ACS lines are utilized to acquire the many GRAPPA kernels, through all the coil images are regenerated and utilized to approximate the coil merging vector. For every realization, the *k*–space coil are non-uniformly subsampled and regenerated utilizing GRAPPA with earlier computed kernel. Finally merged with previous computed merging vector in linear form. Fig 3.6 shows the non-uniform subsampling pattern of VD reconstruction for simulated brain dataset with 32 ACS lines comparing different methods like Monte Carlo, *k*-space and Image-space.

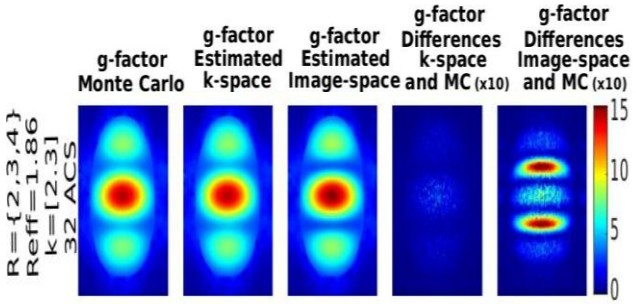

Fig 3.6: Non-uniform subsampling pattern with ACS lines for simulated brain dataset.

4. RESULTS AND CONCLUSION

4.1 RESULTS

Usually image-space will produce two resources of delusion, firstly the reconstructed image in the frequency space is not precisely equal to the reconstructed image in the *k*–space. As soon as the kernel size is applied to a filtering location, the subsistence of the outcome overlays with other parallel locations, which leads to remaining delusions. As a result, two locations will be correlated hence, the image–space analysis is not completely accurate. Since both Monte-Carlo and image-space methods are inaccurate *k*-space analysis is implemented in this proposed methodology. Here the inputs are *k*-space noise matrices Γ and C which are sub-sampling images like GRAPPA kernel and coil merging vector. In both uniform sub-sampling methods, phase encoding dimension are almost equal hence there is no delusion in the approximation of g-factor. Therefore using k-space analysis, noise maps in GRAPPA are calculated which is computed in MATLAB through codes.

4.1.1 Creation of Fourier Transform *k*-space

By applying 2D Fourier transform from image to frequency space (*k*-space), under-sampled *k*-space is generated for all 6 channels where only one sampling is carried. Fig 4.1 shows frequency space transformed using Fourier Transform. The g-factor are determined for each and every channel in phantom image process that is still not reconstructed using GRAPPA. By varying accelerator factor and kernel size, 6 channel under-sampled k-space are obtained. Fourier transform can be applied in any number of dimensions which helps to obtain 2D frequency space and can be reconstructed using 2DFT.

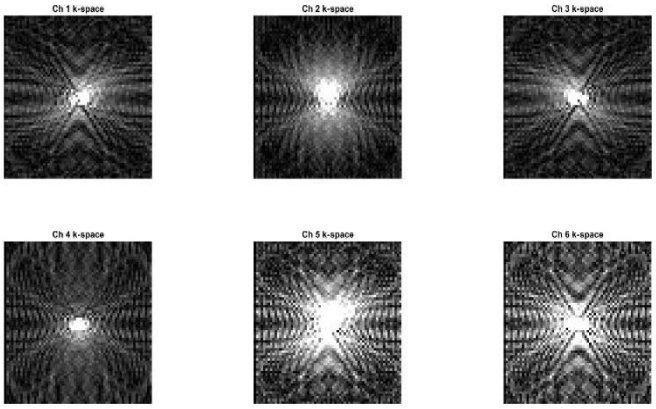

Fig 4.1: Fourier Transform k-space

4.1.2 *k*-space using Auto-calibration lines

Auto Calibration Signals (ACS) are compared with a standard measurement and the measurement using the system. The precision standard measurement are ten times better than that of a measuring signal. Here 16 ACS lines are used from the *k*-space image to estimate the misplaced lines in the image. Fig 4.2 shows auto-calibration lines for all 6 channels.

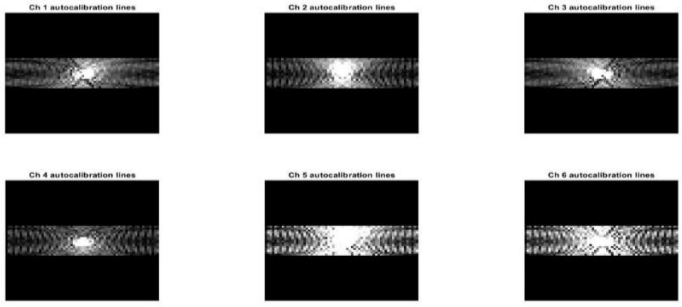

Fig 4.2: Auto-calibration lines in *k*-space

4.1.3 GRAPPA reconstructed image

All the channels are combined using the formula of sum of squares (SOS) which gives GRAPPA reconstructed image. The magnitude and phase of all the channels are combined using SOS method and then the final image is displayed. Fig 4.3 shows the image that is reconstructed using GRAPPA. Increasing kernel size will result in

improvised performance of the reconstructed image with respect to noise amplification.

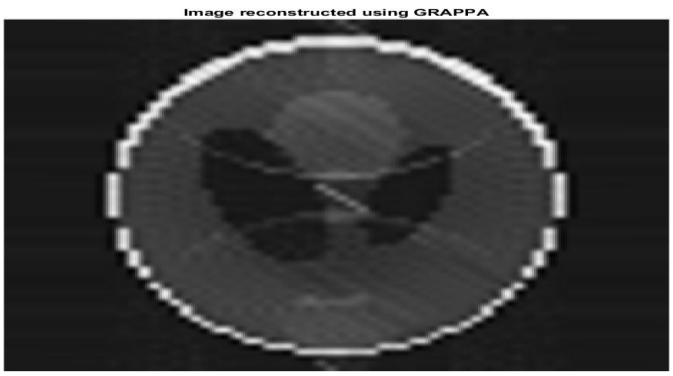

Fig 4.3: GRAPPA reconstructed image

4.2 CONCLUSION

Extra approximations are not required in the proposed methodology although accurate analytical derivation are attained. Since the factual assistance is provided by phantom experiment, other results can be compared with the proposed methodology. Error variation are taken place by varying kernel size, acceleration factor and numerous locations. A computational test that is performed for 256X256 image, image-space technique will require 4.66 seconds wherein *k*-space analysis technique will require 4.06 seconds. This can be achieved by accounting high degree parallelism in regeneration steps.

REFERENCES

[1] S. Aja-Fern´andez and G. Vegas-S´anchez-Ferrero, Statistical Analysis of Noise in MRI. Modeling, Filtering and Estimation. Springer International Publishing, 2016.

[2] E. Saritas, J. Lee, and D. Nishimura, "SNR- dependence of optimal parameters for apparent diffusion coefficient measurements," IEEE Trans. Med. Imag., vol. 2, pp. 424–437, 2011.

[3] D. Collins, A. Zijdenbos, V. Kollokian, J. Sled, N. Kabani, C. Holmes,band A. Evans, "Design and construction of a realistic digital brain phantom," IEEE Trans. Med. Imag., vol. 17, no. 3, pp. 463–468, Jun. 1998.

[4] N. Seiberlich, F. Breuer, R. Heidemann, M. Blaimer, M. Griswold, and P. Jakob, "Reconstruction of undersampled non-cartesian data sets using pseudo-cartesian grappa in conjunction with grog," Magn. Reson. Med., vol. 59, p. 11271137, 2008.

[5] S. Aja-Fern´andez, G. Vegas-S´anchez-Ferrero, and A. Trist´an-Vega,n"Noise estimation in parallel MRI: GRAPPA and SENSE," Magn. Reson. Imag., vol. 32, no. 3, pp. 281–290, 2014.

[6] E. McVeigh, R. Henkelman, and M. Bronskill, "Noise and filtration in magnetic resonance imaging," Med. Phys., vol. 12s, pp. 586–591, 1985.

[7] M. Griswold, P. Jacob, R. Heidermann, M. Nittka, V. Jellus, J. Wang. Kiefer, and A. Haase, "Generalized autocalibrating partially parallel acquisitions (GRAPPA)," Magn. Reson. Imag., vol. 47, pp. 1202–10, 2002.

[8] P. Th¨unberg and P. Zetterberg, "Noise distribution in SENSE- and GRAPPA- reconstructed images: a computer simulation study," Magn. Reson. Imag., vol. 25, pp. 1089–94, 2007.